Separation Science and Technology
Publication details, including instructions for authors and subscription information:
http://www.informaworld.com/smpp/title~content=t713708471

A Rapid Analysis of Ultrafiltration Membrane Structure

A. N. Cherkasov[a]
[a] State Institute of Highly Pure Biopreparations, St.-Petersburg, Russia

To cite this Article Cherkasov, A. N.(2005) 'A Rapid Analysis of Ultrafiltration Membrane Structure', Separation Science and Technology, 40: 14, 2775 — 2801
To link to this Article: DOI: 10.1080/01496390500333111
URL: http://dx.doi.org/10.1080/01496390500333111

Separation Science and Technology, 40: 2775–2801, 2005

ISSN 0149-6395 print/1520-5754 online
DOI: 10.1080/01496390500333111

A Rapid Analysis of Ultrafiltration Membrane Structure

A. N. Cherkasov
State Institute of Highly Pure Biopreparations, St.-Petersburg, Russia

Abstract: The possibility of using protein calibration data for rapid analysis of ultrafiltration membrane structure is discussed. It is shown that structure analysis based on calibration data gives the possibility of determining the mean membrane pore radius, and the view of distribution of pores by size, to reveal and to asses the microscopic membrane defectness, to estimate the thickness of selective layer, and also to correlate the structure of investigated membrane with that of the principal serial ultrafilters. Beside this, the use of permeability data obtained during protein calibration gives the possibility to assess the hydrophilicity of membrane investigated. However, the principal advantage of this method is high productivity and the possibility to perform the analysis with the use of the simplest ultrafiltration and gel chromatographic equipment. The examples of the use of membrane structure analysis in the course of development of composite polysulphoamide membranes and track-etched ultrafilters are given.

Keywords: Ultrafiltration, membrane structure, pore size, distribution of pores by size, defectness, thickness of selective layer, hydrophilicity

INTRODUCTION

Have you ever noticed that whereas numerous methods of membrane structure analysis exist, at the present time it is hardly possible to find in literature the papers in which these methods are applied to the routine structure analysis in the course of membrane development or manufacturing (i.e., in the cases when

Received 2 February 2005, Accepted 1 September 2005
Address correspondence to A. N. Cherkasov, State Institute of Highly Pure Biopreparations, Pudozhskaya st. 7, St.-Petersburg, Russia 197110. Tel.: (812) 230-47-36; Fax: (812) 230-49-48; E-mail: aculina@vc3709.spb.edu

it is necessary to analyze a large number of membrane samples in a restricted time)?

This can be attributed to the following two factors:

1. The existing methods are not accessible for this purpose either because of long measurement duration or because of the necessity to use laborious and expensive equipment.
2. The often-existing need for the interpretation of the results obtained in membrane analysis in terms of structure parameters and operating characteristics, i.e., the investigation methods, very often get transformed into the objects of investigation (1, 2).

Considering these factors, the method of structure analysis based on protein calibration seems to be quite irreplaceable. Except for detecting such standard membrane operating characteristics as molecular weight cut-off (MWCO) and the width of retention curve, this method suggested by us earlier (3, 4) delivers the possibility to determine the mean pore radius, and the view of distribution of pores by size. It also allows to reveal and assess the nature of microscopic defects, to estimate the thickness of selective layer, and to compare the investigated membrane to principal types of serial ultrafilters by structure.

In spite of the multiple benefits listed, the principal advantage of this method is definitely its high productivity. That makes it truly irreplaceable for rapid structure analysis. Thus, the use of structure analysis based on protein calibration allows a medium qualification researcher to investigate up to a dozen membranes per day.

In summary, the purpose of this review is to demonstrate the capabilities of calibration method for rapid analysis of membrane structure. To illustrate the efficiency of this method, its application for structure analysis of polysulfonamide UF membranes and asymmetric track-etched ultrafilters in the process of their development will be discussed.

However, before proceeding to discuss the use of calibration data for analysis of membrane structure it is necessary to briefly recall the principal concepts of selective behavior of UF membranes in protein ultrafiltration as well as the principal regularities of membrane calibration procedure.

PROTEIN ULTRAFILTRATION

It is known that the principal peculiarity of protein ultrafiltration is the determining influence of gel formation on membrane permeation and selective[1] properties. Although the existing models of concentration polarization (CP)

[1]By selective properties we mean the ability of ultrafiltration membrane to separate the solutes differing in molecular masses (sizes of molecules).

(such as gel-polarization model (5), boundary layer resistance model (6, 7), osmotic pressure model (8), or different combination of these models) describe the changes of membrane permeability sufficiently well, they do not even consider the regularities of selective behavior of UF membranes in the course of gel formation. The only model which describes the selective behavior of UF membranes during protein ultrafiltration is the polarization-sieving (PS) model proposed by us earlier (3, 9). According to this model, in the process of ultrafiltration a gel layer decreasing the sizes of all pores by a constant value ΔR appears on the membrane surface (Fig. 1).

At the same time, the sieving mechanism still exists in the reduced (by 2 ΔR) pores. Along with the growth of gel layer (caused, for example, by increasing of bulk concentration or transmembrane pressure), the increase of ΔR takes place, which causes a shift of retention curves toward low molecular weights (Fig. 2).

Although it was supposed first that during gel formation all pores are reduced by a constant value $2\Delta R$ which depends only on CP level, the latest investigation (10) demonstrated that ΔR value is linearly, proportional to pore size. In particular, this conclusion explains the preservation of logarithmic normality and width of retention curves and their shifting toward low M with CP rise (see Fig. 2). One can think that the direct proportionality between ΔR and R is caused by very low effective porosity (f_0) of modern ultrafiltration membranes ($f_0 \sim (10^{-1} - 1)$ %) (11, 12). As a result of this low porosity, the CP level for an individual pore is determined not by a total solute flux to membrane surface but by a separate flux through this pore, i.e., by its size.

Further refinement of polarization-sieving model carried out in (13) also showed that gel layer decreasing the pore sizes must be considered as a superposition of reversible and irreversible adsorption layers (Fig. 1). The ratio of the thicknesses of these layers is determined by membrane and solute hydrophilicities.

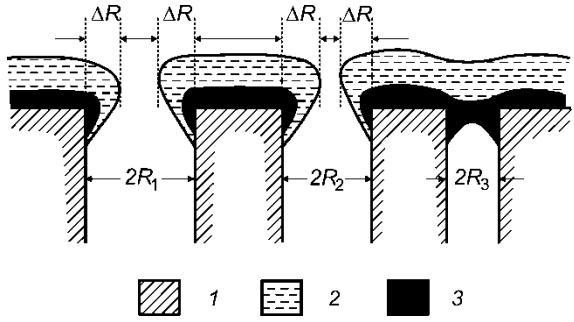

Figure 1. Formation of gel layer on UF membrane surface according to polarization-sieving model. 1–membrane material, 2–layer of reversible protein adsorption (gel-polarization layer), 3–layer of irreversible protein adsorption (3, 9, 13).

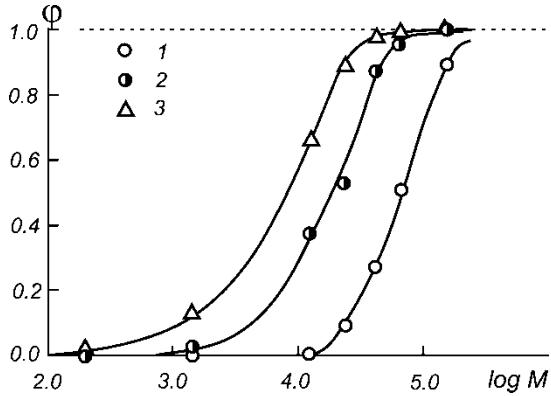

Figure 2. The shift of retention curves of membrane Omega-100 (Gelman) obtained in the process of CP rise caused by transmembrane pressure (Δp) increase: 1–Δp = 0.2 bar, 2–Δp = 1 bar, 3–Δp = 2 bar. Concentration rate K = 1.1 (10).

CALIBRATION PROCEDURE

The selective properties of UF membranes are characterized by retention curve, i.e., by the dependence of observed retention coefficient (φ)

$$\varphi = 1 - (C_P/C_B) \tag{1}$$

where C_P and C_B are the concentrations of permeate and bulk, respectively) on molecular weight (M) of the solute (φ(M). The molecular weight of a globular protein with the retention coefficient equal to 90% is called the molecular weight cut-off (MWCO) (M_L).

Best of all the membrane protein calibration (determination of membrane retention curve) can be carried out by passing through membrane model mixtures of globular proteins and low molecular substances with gel chromatographic analysis of permeate and bulk concentrations (Fig. 3). The compositions of model mixtures used for analysis of UF membranes with different MWCO values are listed in Table 1.

As it follows from above, the results of calibration procedure are substantially determined by concentration polarization level, i.e., by the conditions in which the calibration is performed. Therefore, in order to determine membrane structure characteristics one must use data obtained in more or less "standard" calibration conditions (cells with laminar stirring, (200–600) min^{-1}, calibration with globular proteins at concentration of $\sim 10^{-1}$%, pressure $\approx$1bar, permeate samples must be taken after passage of approximately 1 cm^3 of permeate through 1 cm^2 of membrane area[2]).

[2]The last condition must ensure the establishment of stationary permeate flow, i.e., the formation of equilibrium gel layer on membrane surface.

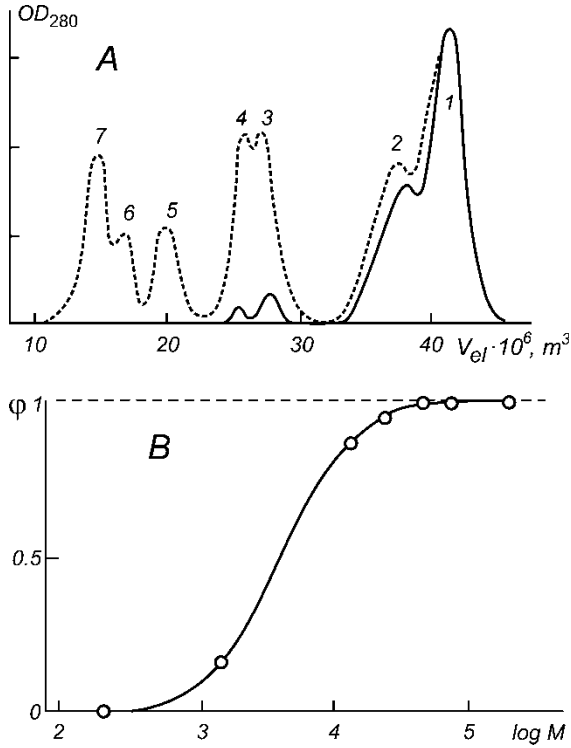

Figure 3. Procedure of membrane protein calibration: (A) Gel chromatograms of initial solution of model mixture consisting of 1–tryptophan, 2–bacitracin, 3–cytochrome-C, 4–chymotrypsinogen, 5–ovalbumin, 6–bovine serum albumin, 7–γ-globulin, (dotted line), and permeate (solid line) obtained on membrane UAM-150, OD_{280} is optical density at 280 nm. (B) Membrane UAM-150 retention curve plotted from chromatograms Fig. 3A. (3, 14).

In particular, the use of "standard" calibration conditions allows us to compare the structure parameters and operating characteristics of membranes under investigation to those of serial ultrafilters (see the section "The Analysis of the Structure of Track-Etched Ultrafilter").

THE USE OF CALIBRATION METHOD FOR ULTRAFILTRATION MEMBRANE STRUCTURE ANALYSIS

Determination of Average Pore Size and Distribution of Pores by Size

The determination of average pore size of UF membranes is based on the existence of empirical relationship [the so-called "critical ratio" (λ_{cr})]

Table 1. Model mixtures used for TEUF calibration (M–molecular weight and r_S–Stokes' radius of protein, pI–protein isoionic point) (3, 14)

	N	M 10^3, g/mol	r_S,	pI	*a*	*b*	*c*
1	Tryptophan	0.204	3.7	—	+	+	
2	Bacitracin	1.45	8.3	7.1–7.2	+		
3	Vitamin B_{12}	1.36	7.8	—		+	
4	Cytochrome C	12.4	17.6	10.6	+	+	+
5	Chymotrypsinogen	24.0	22.7	9.5	+	+	+
6	Ovalbumin	44.0	28.6	4.6		+	+
7	Bovine serum albumin	67.0	34.0	4.7		+	
8	γ-globulin	160.0	46.5	7.1		+	+
9	Catalase	232.0	53.5	5.4–5.7			+
10	Ferritin	440.0	68.0	—			+
11	Thyroglobulin	690.0	83.0	4.5			+

[a]Low molecular mixture (MWCO ÷ (100–20 000) g/mol), ($C_\Sigma \approx 0.12\%$).
[b]Middle molecular mixture (MWCO ÷ (100–200 000) g/mol), ($C_\Sigma \approx 0.6\%$).
[c]High molecular mixture (MWCO ÷ (5000–1 000 000) g/mol), ($C_\Sigma \approx 0.6\%$).

between the minimal Stokes' radius of protein molecule effectively retained by membrane (r_L) and mean hydrodynamic pore radius (R_h) brought out by Elford in 1937 (15)

$$\lambda_{cr} \equiv r_L/R_h \tag{2}$$

The determination of critical ratio was carried out in (16, 17) for UF membranes of homogeneous structure, which gave the authors the possibility to calculate R_h values from Hagen-Poiseuille equation. The MWCO values were used as molecular weights of proteins retained effectively by membrane. The r_L values were determined with the help of equation of Mark–Kuhn–Hawink type for globular proteins (3)

$$r_L = K_1 M_L^b \tag{3}$$

where $K_1 = 0.49\,\text{Å}(\text{mol/g})^b$ and $b = 0.38$ are constants.

In (18, 19) the values of λ_{CR} were determined for asymmetric membranes. In order to do this the authors used the electron microscopy data on pore sizes and distributions of pores by size obtained for membranes of asymmetric structure in (12, 20, 21). For determining the critical ratio for homogeneous membranes Poiseuille radius with averaging of the form 4 was used

$$R_h = \left(\frac{\int_0^\infty f(R)R^4 dR}{\int_0^\infty f(R)R^2 dR}\right)^{1/2} = R_0 e^{\sigma_0^2} \tag{4}$$

where $f(R)$ is the differential numerical pore size distribution function, R_0 is the pore radius corresponding to the maximum of the PSD function, and σ_0 is PSD dispersion. The same averaging was used for asymmetric membranes.

Thus, as it follows from the data (15–19) for ultrafiltration membrane of arbitrary structure a universal relationship between mean hydrodynamic pore radius and radius of a particle (molecule) with retention coefficient equal to 90% exists

$$\lambda_{cr} \equiv (r_L/R_h) = 0.30 \pm 0.15 \tag{5}$$

The values of λ_{cr} are less than unity because the sizes of membrane pores are reduced in the process of protein ultrafiltration by gel layer (see Fig. 1). Therefore, the molecules with sizes less than pore radius can be retained by membrane.

The existence of critical ratio allows to determine average pore size of membrane. In order to do this it is necessary to determine the MWCO value and to estimate the value of R_h by equation

$$R_h = K_1 \lambda_{cr}^{-1} M_L^b \tag{6}$$

It is essential to notice that expression similar to eq. (6) was obtained by Sarbolouki (22) for determination of membrane pore size from dextran retention coefficients. Pore radii were determined by the calibration dependence corresponding to the value of $\lambda_{cr} = 1.4$ (19). In the case of dextran ultrafiltration a high rate of λ_{cr} seems to be predetermined by the absence of gel polarization (and therefore of pore overlapping), as well as by the application of the number average, and not the mean hydrodynamic pore radius.

As follows from (19), experimental error of λ_{cr} is determined mainly by the influence of membrane surface roughness on the level of concentration polarization and hence on overlapping of pores by gel layer. Therefore, when membranes under analysis are more or less uniform in surface structure (in the case of membrane development or manufacturing, for instance) one can expect that relative changes in membrane pore sizes will be determined more preciously.

As an example of the use of eq. (6) pore radii of homogeneous track-etched ultrafilters determined by this equation (R_h) in comparison with pore radii determined by Hagen–Poiseuille equation (R_P) and also given by manufacturer (R_0)[3] are listed in Table 2.

According to this table, there is a good enough agreement between R_i values obtained by different methods for membranes with MWCO $< 10^6$ g/mol. In the case of higher MWCO, R_h values are overestimated, which is caused, evidently, by the imperfectness of extrapolation procedure.

Since the retention curve is nothing else but the cumulative function of pore size distribution by retention ability, one has a principal possibility to

[3]The values of R_0 were determined by manufacturer by gas permeability.

Table 2. The comparison of pore radii of homogeneous track-etched ultrafilters determined by eq. (6) (R_h), by Hagen–Poiseuille equation (R_P), and given by manufacturer (R_0) (17)

N	R_0, nm	$J_0\ 10^6$, m/s (1 bar)	R_P, nm	$M_L\ 10^{-3}$, g/mol	R_h, nm
1.1	10	2.8	12	60	10 ± 5
1.2	15	5	14	180	15 ± 7
1.3	15	5	14	130	13 ± 6
1.4	15	4.6	13	100	12 ± 6
1.5	15	4.7	13	67	10 ± 5
1.6	20	3.1	12	560	23 ± 11
1.7	20	4	13	70	11 ± 5
1.8	25	45	25	1300[a]	(31 ± 15)
1.9	25	17	19	1500[a]	(33 ± 16)
1.10	25	36.3	22	1300[a]	(31 ± 15)
1.11	35	140	33	—	—
1.12	35	250	33	—	—
1.13	40	162	32	—	—
1.14	45	260	37	—	—

[a]The MWCO values were obtained by extrapolation of retention curves to $\varphi = 0.9$.

evaluate PSD function from calibration data. Mathematically the relation between $\varphi(M)$ and PSD function for UF membrane functioning in GP regime is given by an evident equation

$$\varphi(M) = \frac{\int_{\Delta R}^{\infty} f(R)(R - \Delta R)^4 \varphi[r(M)/(R - \Delta R)]dR}{\int_{\Delta R}^{\infty} f(R)(R - \Delta R)^4 dR} \tag{7}$$

where $f(R)$ is a differential PSD function, $\varphi[r(M)/(R - \Delta R)] \equiv \varphi(\lambda)$ is a sieving function, and ΔR is a value of pore radius reduction by gel polarization (Fig. 1).

According to Ferry's suggestion, made as early as in 1936 (23), the sieving function is determined by molecule accidental hitting a pore in the course of Brownian motion (the so-called steric factor). The most widespread expression for steric factor is of the form:

$$\varphi(\lambda) = [1 - (1 - \lambda)^2]^2 \tag{8}$$

It appeared, however, that Ferry's equation is not supported by experimental results (24). Thus, the retention curve calculated by eq. (8) for a membrane with pores monodisperse by size appeared to be an order of magnitude wider than the experimental retention curves for membranes with absolutely narrow PSD function. As membranes of this kind, Sleytr and Sara membranes (25, 26) made from surface layers (s-layers) of cell envelope of thermophilic bacteria were used. Since s-layers play a role of

ultrafilters in cell envelope, these layers being perfected in the process of evolution, obtained the structure optimal for UF separation. Thus, except high porosity (~50%) and low selective layer thickness (~10 nm) these membranes have absolutely monodisperse PSD with regular channels formed by protein crystals.

To illustrate these examples Fig. 4 presents the comparison of experimental retention curves of Sleutr and Sara membranes (points 1 and 2) with theoretical retention curve (dashed line) plotted according to eq. (8) Thus, it was concluded that the separation mechanism of ultrafiltration has essentially sharper character than Ferry's diffusive mechanism. Therefore, the experimentally proved existence of membranes with retention curves much tightly than predicted by Ferry's mechanism is indicative of the fact that this mechanism is not conceptually correct.

It is likely that ultrafiltration separation mechanism is to be described by the two-pore model (5, 27, 28), i.e., pores transmit or retain solute depending on whether solute size is less or more than pore, respectively. So, if this conclusion is right the steric factor can be ignored and the retention curve can be considered as authentic enough mapping of PSD function.[4]

The most evident assessment of PSD function width can be made from the width of retention curve [from retention curve dispersion (σ) or dispersion coefficient (Δ)]. For logarithmically normal function, which is usually used to describe UF membrane retention curves (31, 32),[5] we have:

$$\Delta = \sqrt{e^{\sigma^2} - 1} \tag{9}$$

A comparison of retention curves for membranes of different types showed a sufficient, an order of magnitude, difference in Δ values (3) that argues for a great variety of UF membrane structure. Thus Δ values can change from 10^{-1} (Sleytr and Sara membranes) up to ~10 for synthetic polymeric membranes (3, 24).

Investigation of Defective Ultrafiltration Membranes

An important area of the study of porous structure aimed at the creation of perfect UF membranes is the revilement of microscopic defects distorting

[4]One must say that this assumption is usually not explicitly used in investigations devoted to the determination of membrane PSD from retention experiments [see, for instance (29, 30)].

[5]The logarithmic normality of UF membranes retention curves is a direct consequence of logarithmic normality of distribution of membrane pores by size in combination with a rigorous sieving mechanism. In its turn, logarithmically normal distribution by size is characteristic of disperse systems of condensation type (fog, smog, hoarfrost, snowflakes, etc.) to which porous polymeric membranes relate.

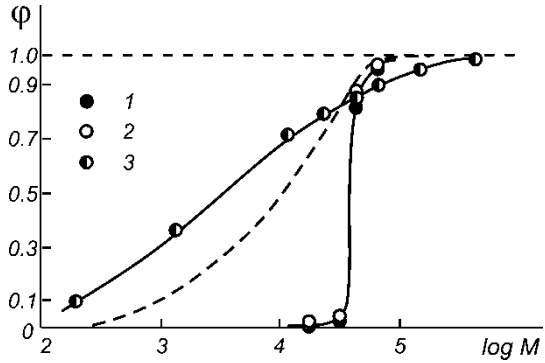

Figure 4. The retention curves of UF membranes differing in PSD width. 1 and 2–Membranes NRS 1536/3C and PV-72 with absolutely monodisperse PSD function obtained by using surface layers of cell envelopes of thermophilic bacteria (26) and dashed line is Ferry's curve for membrane with monodisperse PSD ($M_L = 40\ 10^3$ g/mol), 3–Homogeneous track-etched UF membrane 1.3 obtained by traditional technology (4, 17).

membrane selective characteristics (33–35). These defects can be successfully detected with the use of protein calibration procedure (36).

In general case a defective membrane is characterized by the bimodal PSD function

$$f(R) = f_1(R) + f_2(R) \tag{10}$$

where $f_1(R)$ and $f_2(R)$ are the differential PSD functions of selective and defective membrane pores, respectively.

A characteristic feature of defective membranes is the fact that the size distributions of selective pores and defects do not overlap.

By substituting eq. (10) to the expression for the retention curve of the ultrafiltration membrane working in the gel polarization regime eq. (7) and taking into account that defects are much larger than selective pores, one can obtain for the defective membrane (36):

$$\begin{aligned}\varphi^*(M) &= \frac{\int_{\Delta R}^{\infty} f_1(R)(R-\Delta R)^4 \varphi[r(M)/(r-\Delta R)]dR}{\int_{\Delta R}^{\infty} f_1(R)(R-\Delta R)^4 dR} \\ &\times \left[\frac{\int_{\Delta R}^{\infty} f_1(R)(R-\Delta R)^4 dR}{\int_{\Delta R}^{\infty} f_1(R)(R-\Delta R)^4 dR + \int_0^{\infty} f_2(R)R^4 dR_1}\right] \\ &= \varphi(M)\left(\frac{J_1}{J_1+J_2}\right) \equiv \varphi(M)(1-D_2)\end{aligned} \tag{11}$$

where $\varphi^*(M)$ and $\varphi(M)$ are the retention curves of the defective membrane and its selective pores, respectively, J_1 and J_2 are fluxes through the selective pores

and defects, respectively, and D_2 is the quantitative parameter of membrane defectness which is equal to the ratio of fluxes through defects to total flux through membrane (Fig. 5).

As it can be seen from eq. (11), the retention curve of the defective membrane repeats the retention curve of selective pores with an accuracy of a constant factor determined by the ratio of fluxes through the selective pores and defects. From the above, it follows that, based on the calibration data for the defective membrane, it is possible to establish such characteristics of its selective pores as the MWCO and the dispersion of the retention curve. M_L and σ are determined by a standard method after normalizing the retention curve $\varphi^*(M)$ to 1 (Fig. 5).

The analysis of defectness of polysulfonamide UF membranes was carried out in (36, 37) by calibration method and by comparison of the data obtained with membrane defectness determined by liquid displacement (LDM) and scanning electron microscopy (SEM) methods. The retention curves of membranes 22, 23, and 24 with different extents of defects are shown in Fig. 6.

As shown in Fig. 6, membrane 22 has a usual retention curve reaching the values of $\varphi = 1$ at $M \approx 10^5$ g/mol, which indicates the absence of defects. This conclusion is confirmed by analysis of this membrane by liquid displacement method and by electron microscopy (see Table 3).

The retention curve of membrane 23 achieves the plateau value of φ equal to 0.4, which points to the presence of the macroscopic defects with the value of $D_2 = 0.6$. This evaluation agrees with the data of LDM and SEM according to which this membrane is characterized by the presence of defects within the size range of 0.3–0.5 μm (Table 3).

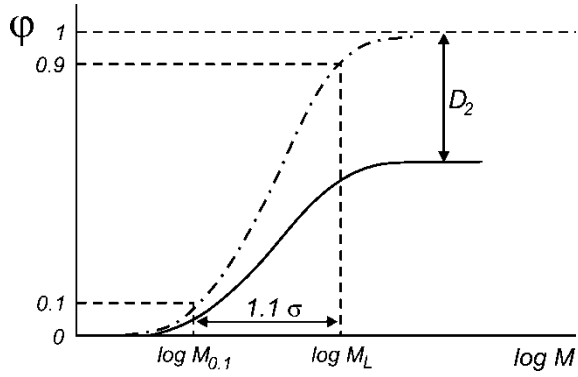

Figure 5. The retention curve of defective membrane (solid line) and the retention curve of selective pores of this membrane (dashed-dotted line), M_L is MWCO, M_{01} is molecular weight corresponding to 10% retention, and σ is dispersion of retention curve of defective membrane selective pores (36).

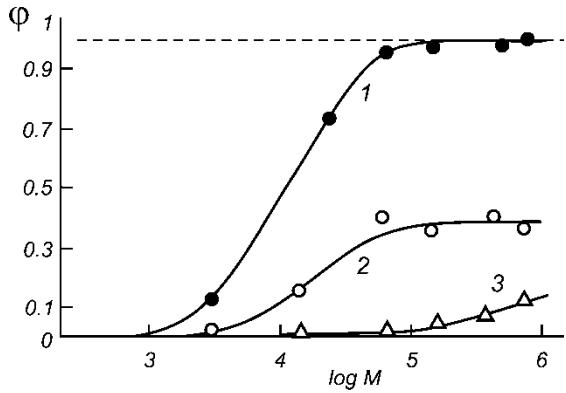

Figure 6. The retention curves of membranes: 1–22, 2–23, and 3–24 with different levels of defects (36).

Finally, membrane 24, to be absolutely precise, does not fall under the definition of the "defective" one, since it has no pores with the sizes characteristic of ultrafiltration membranes (the retention curve does not achieve the plateau value up to $M \sim 10^6$ g/mol). That is why this membrane can be considered as one of the membranes of the microfiltration type with wide PSD function. This conclusion also corresponds to the data of check methods. The pore size distribution for this membrane extended to the region of sizes typical for microfilters (0.2–1.6 μm) (Table 3).

Table 3. Results of analysis of defects in samples of composite membranes on polypropylene (PP) and lavsan (LN) supports with MWCO values close to the critical M_L values (36)

Membrane number	Support	$M_L\ 10^{-3}$, g/mol	D_2	$\Pi_2{}^a$ (size of defects)	SEM
9	PP	45	0	—	Defects are absent
22	PP	60	0	0	Defects are absent
17	PP	65	0.65	—	Defects are present
23	PP	70	0.6	0.1 [(0.3–0.5) μm]	Defects are present
18	PP	75	0.3	—	—
21	LN	45	0	—	Defects are absent
19	LN	90	0	—	—
20	LN	100	0	—	Defects are absent
24	LN	>100	1.0	1.0 [(0.2 – 1,6) μm]	High defectness

[a]Π_2 is the quantitative assessment of membrane defectness in liquid displacement method similar to D_2 value in membrane calibration.

Use of Selective and Permeable Characteristics for Determination of Thickness of Ultrafiltration Membrane Selective Layer

Although the thickness of selective layer (l_S), along with pore size, is a principal characteristic of membrane structure, the determination of l_S is one of the most complicated problems in ultrafiltration. The complexity of this study is predetermined by an uncertainty of the very notion of selective layer, as well as by the model character and high labor consumption of the current methods of l_S determination [see, for instance, (11)]. However, the use of calibration data gives the possibility to assess the thickness of selective layer (3).

Thus, substituting eq. (5) in the Hagen-Poiseuille's equation and using the interdependence between the Stokes' radius and molecular weight of the globular protein eq. (3), eq. (12) was obtained (3). It gives the possibility to determine the reduced thickness of selective layer (l_S/f_o) from membrane selective and permeable characteristics.

$$J_o = K_2 \left(\frac{l_S}{f_o}\right)^{-1} M_L^{0.76} \tag{12}$$

where J_o is water flux at 1 bar, $K_2 = 1.96\ 10^{-13}\ (g/mol)^{-0,76}\ m^2/s$ is a constant, and f_o is the effective porosity.

Being determined by eq. (12), the value (l_S/f_0) is averaged in the form

$$\frac{l_S}{f_o} = R_h^2 \sum \frac{1}{R_{hi}^2} \left(\frac{l_{Si}}{f_{oi}}\right) \tag{13}$$

where the summarizing is carried out by the membrane layers (l_{si}) which have constant pore radius R_{hi} and porosity f_{oi}.

The error of (l_S/f_o) determination comprises the error of critical ratio $\sim$50%, the error of flux determination $\sim$10% and the error of MWCO value $\sim$(30–40%). So, the estimation of selective layer thickness can be carried out with twofold error. If one takes into account that l_S lies in the range of about 5 orders of magnitude (from 10^2 mcm for homogeneous to 10^{-3} mcm for highly asymmetric membranes) this accuracy of selective layer determination can be accepted as quite satisfactory.

A great advantage of eq. (12) is in its universal character since determination of the (l_s/f_o) value is carried out using the filtration methods that fit the analysis of any type of the ultrafiltration membranes.[6]

At the same time eq. (12) is the basis of the modern system of UF membrane classification on the thickness of selective layer (39). Thus, if the data for the series of membranes with constant l_S/f_o value is plotted on the

[6]For instance, in (38) eq. (12) was successfully used for analysis of dynamic viral-protein membrane which appeared in the course of anti-influenza vaccine microfiltration.

classification diagram which consists of log J_0(log M_L) plot all the points must fit a straight line with a slope of 0.76 to abscissa axe. A line AB normal to the series of lines reflecting the constant selective layer thicknesses serves as the axis for (l_S/f_o) parameter (Fig. 7). This diagram based only on selective and permeable membrane characteristics allows comparing the arbitrary membranes by their structure properties.

When permeability coefficients and MWCO values of principal series of commercial membranes have been plotted on a classification diagram an interesting regularity has been revealed. It was found that the points corresponding to every membrane series fit a straight line of a constant (l_S/f_o) value, i.e., membranes of one series are characterized, as a rule, by a constant value of reduced selective layer thickness (see Fig. 7).

Taking into account that effective porosity of homogeneous ultrafilters is about 50% (3, 18) and that of highly asymmetric membranes reaches a tenth of a percent (12), one can see that the selective layer thickness varied between 100 μm (homogeneous membranes Sartorius SM, Biopore UAM) and 10^{-3} μm (highly asymmetric membranes Diaflo PM, Gelman Omega).

Since only selective and permeable membrane characteristics are used for diagram plotting one has a possibility to pictorially compare an arbitrary membrane with principal ultrafilters of commercial series.

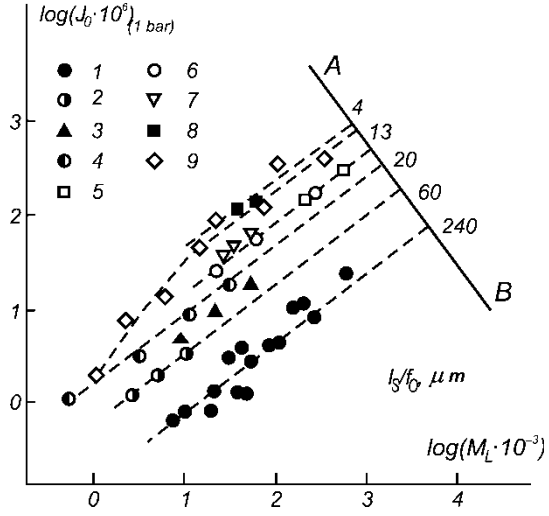

Figure 7. Diagram of classification of UF membrane series by the reduced thickness of selective layer: 1–Sartorius SM 115-117, and Vladipore UAM, 2–Biopore A2-10, 3–DDS-5,600, -800, 4–Diaflo UM, 5–Biopore A-20-500, 6–Diaflo XM, 7–Dorr-Oliver XP, 8–Diaflo PM, 9–Gelman Omega (3, 39).

The Assessment of Ultrafiltration Membrane Hydrophilicity

It is convenient to characterize UF membrane hydrophilicity by the value of flux recovery ratio (FRR) (40)

$$FRR = J_{ot}/J_o \tag{14}$$

where J_o–water flux before ultrafiltration and J_{ot}–water flux after protein calibration and membrane washing.

As remarked, (Fig. 1) in the process of gel polarization, gel layer appearing on membrane surface consists of a layer of irreversibly sorbed polymer and of a layer of gel polarization. As a result of membrane washing the gel polarization layer dissolves, membrane permeability increases, and now is determined only by the thickness of irreversibly adsorbed polymer layer. In its turn, the thickness of adsorbed polymer layer is determined by membrane and solute hydrophilicities. However, as the very notion of irreversible adsorption is relative (in any case one can find a detergent strong enough to clean membrane completely), it is very important for the washing procedure to be standard. As it seems to us, it is the most convenient to use the washing procedure proposed by Nilson (40). This procedure consists of a membrane washing in water and buffer with intensive stirring for 1 min each.

FRR values for membranes of different hydrophilicities after calibration by model protein mixtures have been determined in (13). As it follows from this study, for ultimate hydrophilic membranes made from regenerated cellulose, FRR value reaches 1.0 (complete recovery), for hydrophilic membranes from cellulose, acetate and polyamide imide FRR $= 0.5 \pm 0.1$ and for membranes made from moderately hydrophobic polysulfonamide FRR $= 0.4 \pm 0.2$. It is interesting to notice that permeability recovery after membrane washing correlates with recovery of membrane selective properties, as it follows from polarization sieving model.

EXAMPLES OF PRACTICAL USE OF RAPID STRUCTURE ANALYSIS FOR DIFFERENT TYPES OF ULTRAFILTRATION MEMBRANES

Structure Analysis of Composite Ultrafiltration Membranes

In (41) the method of rapid structure analysis was used in the process of development of the composite polysulfonamide membranes obtained on the nonwoven polypropylene (PP) and lavsan (LN) supports.

The membranes were produced by dry-wet method in the range of casting solution concentration 5–14%. The aim of the research was to analyze the nature of defects which appeared in experimental membrane samples.

It was suggested that the appearance of defects is caused by the reduction of selective layer thickness with the decrease of casting solution

concentration. To prove this suggestion the dependence of l_s [determined by eq. (12)] on MWCO was plotted. This dependence is shown in Fig. 8. The l_s^* calculation was carried out with the arbitrary assumption that the membrane effective porosity is 10%.

Despite a considerable scatter caused by various conditions of casting of the experimental batches, it is obvious from this figure that one can observe a monotonous decrease in l_S^* value with an increase in the membrane pore size (with decrease of concentration of casting solution). Since a decrease of the selective layer thickness enhances the probability of defect formation, obtaining of l_S^* zero values may be considered as transition from the defect-free to defective ultrafiltration membranes. Thus, the values of M_L, that in Fig. 8 correspond to zero value of the selective layer thickness, are considered in (41) as the limits of the defect-free characteristics of the membranes on two types of supports.

The extrapolation of $l_S(M)$ dependence to zero thickness of selective layer gives the possibility to assess MWCO values corresponding to the limits of the defect-free characteristics of the membranes on two types of supports. The calculation of the limiting MWCO values carried by least-squares technique gives:

$$\begin{aligned} &\lim M_L = (60 \pm 10)10^3\ \text{g/mol} \quad (\text{polypropylene support}) \\ &l_S = 0 \\ &\lim M_L = (100 \pm 20)10^3\ \text{g/mol} \quad (\text{lavsan support}) \\ &l_S = 0 \end{aligned} \tag{15}$$

The analysis of membranes with the values of M_L near the critical rates (15) by liquid displacement method (Π_2[7] and defect pore size), calibration method (D_2), and SEM confirms this conclusion (Table 3).

As follows from the data in Table 3, the structure defects characterized by the value $D_2 = 30–60\%$ really arise for membranes on the polypropylene support when the $M_L = 60\ 10^3$ g/mol is exceeded.

As for membranes on lavsan support, the above-mentioned highly defective membrane 24, characterized by a continuous pore distribution up to several mcm, proved to be the only sample with the value of $M_L > 100\ 10^3$ g/mol. The conclusion about the thinning of the selective layer with MWCO increase is proven by SEM analysis of selective surface of membrane 24. It demonstrates the low thickness of its selective layer leading to appearance of numerous defects (36).

Therefore, the use of the rapid structure analysis method gave the possibility to reveal on-line (in the course of membrane development) the presence of microscopic defects and also to explain the cause of its appearance.

[7]Π_2 value is equal, similarly to D_2, to the ratio of water flux through defects to total water flux through membrane.

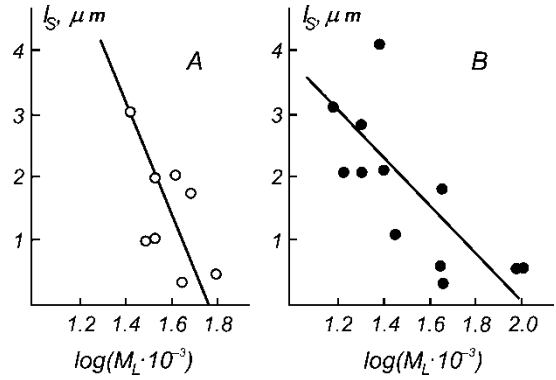

Figure 8. The effective thicknesses of selective layer (l_S^*) of polysulfonamide membranes on polypropylene (A) and lavsan (B) supports vs. MWCO (M_L) (37).

The Analysis of the Structure of Track-Etched Ultrafilters

In (17, 42) the prompt analysis of UF membrane structure based on calibration data was used in the process of development of asymmetric polyethylene terephthalate track-etched ultrafilters (TEUF). The necessity of the development of asymmetric TEUF was caused by extremely imperfect permeable and selective properties of traditional track-etched filters with pores of ultrafiltration size. Thus, the research carried out earlier (43) showed that these membranes are characterized by low permeability as well as a tendency to pore plugging which can be connected with high length of ultrafiltration pores.

Comparative investigation of TEUF of two types was carried out. The membranes of the first type were the homogeneous track-etched filters with cylindrical capillaries obtained by traditional technology. The pore size is determined by the time of etching of a film irradiated previously by accelerated heavy ions or fusion fragments (44). The membranes of the second type were produced by the same technology but with the use of films with preliminary treatment of surface layer (45). Since the etching velocity of treated layer is lower than that of bulk, one can expect to obtain track-etched membranes with asymmetric structure.

As a result of assumption that the tendency to pore plugging can be also caused by the increased adsorption ability of pore material after etching (42) the FRR values characterizing membrane hydrophilicity were measured in the course of membrane calibration. Flux recovery ratios were determined for both types of track-etched ultrafilters. It appears that FRR $= 0.4 \pm 0.1$ which is characteristic of moderately hydrophobic membranes. It dispelled the assumption of increased adsorption ability. The further measurements of adsorption isotherm confirm this conclusion. The amount of protein adsorbed on a unit of pore surface comprises the value of $0.14 \pm 0.04\,\mathrm{mcg/cm^2}$ which is close to literature data for moderately hydrophobic membranes (17).

Altogether more than a hundred of membranes of both types have been investigated. It is important that there was a great variety of pore structures of these membranes. The typical retention curves of TEUF with different structure are presented in Fig. 9.

As shown in this figure, defective UF membranes (curve 2), microfilters (curves 3 and 4), and also membranes with large amount of nanofiltration pores (curves 2 and 4) are present along with usual UF membranes (curve 1).

In some cases membranes of both types were characterized by bimodal retention curves (bimodal PSD distribution) (Fig. 10). For "bimodal" TEUF of the first type the size of tight pores comprises $\sim 100'$ and that of large pores rises from $\sim 100'$ to $\sim 400'$ with the rise of mean pore size. As for the membranes of the second type the size of tight pores was $\sim 50'$ and that of the large $\sim 100'$.

The data obtained in the process of membrane calibration allowed all membranes with imperfect ultrafiltration structure to exclude from consideration, i.e., all membranes of microfiltration type, all defective UF membranes, and all membranes with large (more than 10% by permeability) amount of nanofiltration pores. Thus, only about 60 out of approximately 100 of TEUF samples remained for further structure analysis.

The next peculiarity of TEUF structure that has been found was abnormally wide retention curves of membranes of both types. This fact points to the existence of broad distribution of pores by size (see Fig. 4, curve 3). The broad PSD is very atypical for track-etched filters which are famed for narrow pore size distribution and strictly round pore shape (Fig. 11A). This wide PSD was quite unexpected by the authors because one of the aims of asymmetric TEUF development was to create high selective ultrafiltration

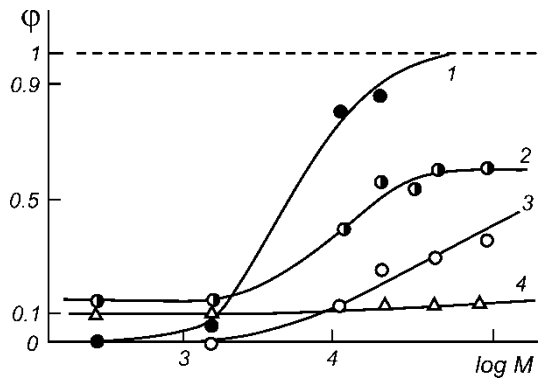

Figure 9. The retention curves of track-etched ultrafilters with different pore structure. 1–Usual UF membrane with MWCO = 20 10^3 g/mol and $\Delta = 1.4$, 2–Defective UF membrane ($D_2 = 0.4$, MWCO = 25 10^3 g/mol) having pores of nanofiltration sizes, 3–Microfiltration membrane, 4–Microfiltration membrane having pores of nanofiltration sizes (17, 42).

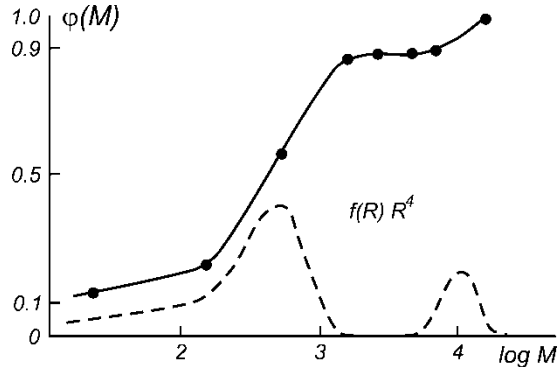

Figure 10. The retention curve of track-etched UF membrane 5.4 (solid line) and approximate curve of pore distribution of this membrane by size (dashed line) (17).

membranes with narrow distribution of pores by size (analogous to membranes of Sleytr and Sara (see previous section). However, as it follows from microphotographs, pore entrances of track-etched UF membranes have a wide range of sizes and irregular, far from round, shape (Fig. 11B). One can think that these peculiarities of membrane structure are caused by the influence of submolecular structure of initial film in which the regions of different densities exist (46). As the etching velocity depends on the density of material, one can expect the appearance of either wide PSD or of irregular pore shape. In the case of track-etched microfilters the sizes of polymer heterogeneity regions are much less than pore sizes and these regions do not have an effect on membrane PSD.

The presence of submolecular polymer structures (crystallites) is well seen on micrographs of TEUF of the first (A) and of the second (B) types (Fig. 12) obtained with the use of atomic force microscope (AFM).

According to these figures the preliminary treatment of polymer film in the process of TEUF production leads to homogenization of polymer structure (the size of submolecular structures decreases). This homogenization leads, in turn, to decreasing of PSD width. Thus, the mean width of retention curves of TEUF of the second type appeared to be twice lower than that of the first type ($\Delta = 2 \pm 1$ and $\Delta = 4 \pm 1$, respectively) (17).

The next step in TEUF structure analysis was the determination of mean pore sizes (see, in particular, Table 2) and the thicknesses of selective layer. These values are the principal structure characteristics of UF membranes.

The performed analysis demonstrated that TEUF of the first type are homogeneous filters with selective layers approximately coinciding with total membrane thicknesses (L). As for TEUF of the second type, the variation of treatment conditions gave the possibility to obtain membranes with pore structure changing from homogeneous [$l_S = \mathrm{L} \div (10\text{–}20)$ μm] to extremely asymmetric ($l_S \sim 10^{-2}$ μm).

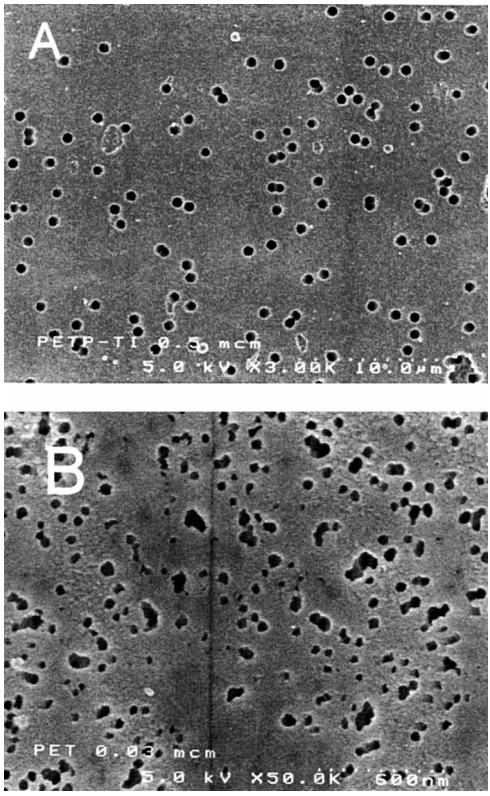

Figure 11. SEM microphotographs of track-etched filters with different pore sizes: A – Track-etched microfilter (R≈0.25 μm), B – Track-etched UF membrane 1.3 (R ≈ 0.015 μm) (17).

The difference in structure of two TEUF types can be best shown by classification diagram Fig. 7. This classification diagram containing the values of water fluxes and molecular weight cut-off for studied TEUF of two types is presented on Fig. 13. The principal advantage of the use of this diagram for TEUF classification is the precious knowledge of the porosity of these membranes, which permits to immediately mark the thickness of the selective layers on the axis AB. The straight lines of constant (l_S/f_o) values from diagram Fig. 7 are plotted on diagram Fig. 13, That makes it possible to compare membranes of different types by its permeable and selective properties.

As it follows from Fig. 13 the points corresponding to membranes of the first type (zone I) arranged about the line of constant selective layer thickness $l_S \sim 10\,\mu m$ which coincides with the total thickness of membrane. This fact illustrates the statement that membranes of this type are really the traditional

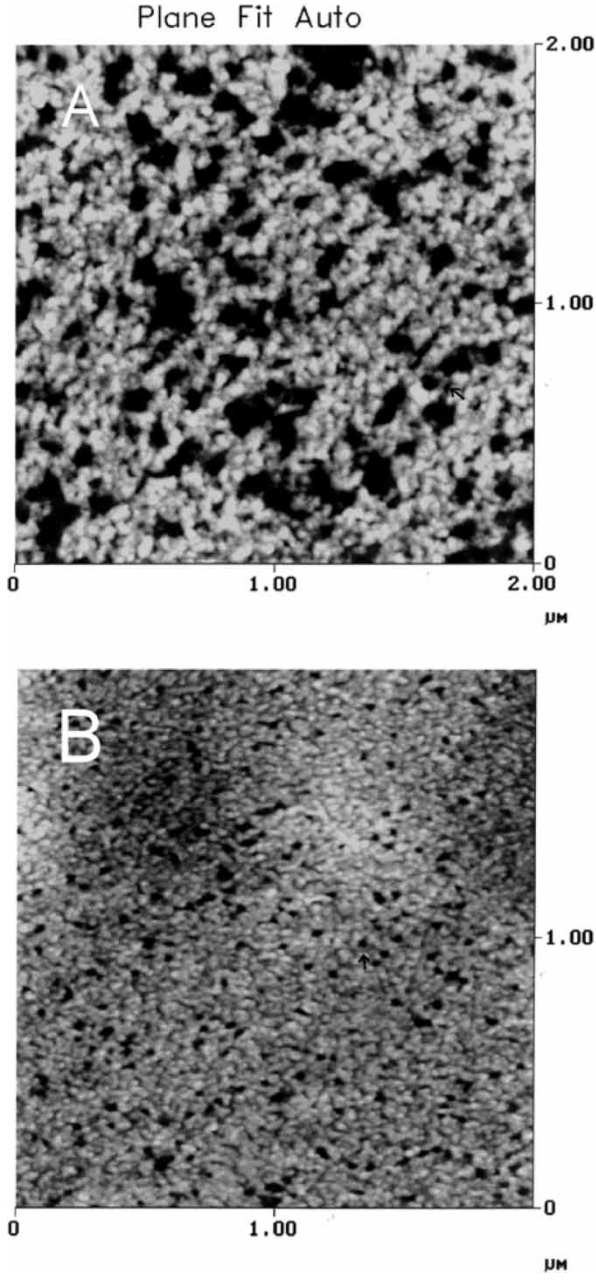

Figure 12. The AFM micrographs of the surfaces of TEUF obtained at equal etching time without (A) and with (B) preliminary treatment of initial film surface. Kindly supplied by Zbynek Pientka (Institute of Macromolecular Chemistry AS CR, Prague, Czech Republic).

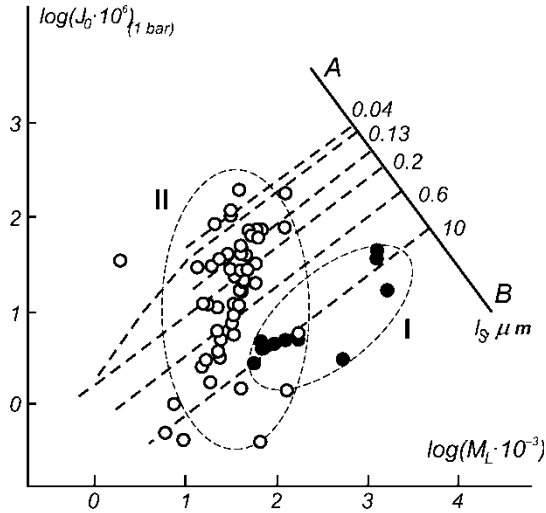

Figure 13. Diagram of classification of track-etched ultrafilters by the thickness of selective layer. Zone I corresponds to TEUF of first type and zone II to TEUF of second type. Dashed lines correspond to lines of constant (l_S/f_0) parameter Fig. 7. (17, 42).

track-etched filters with cylindrical capillaries passing through whole membrane thickness.

The membranes of the first type correspond to the old low permeable membranes with homogenous structure (Vladipore, UAM, Sartorius SM-115-121) by permeability. One can think that the tendency of these membranes to fouling as well as their bad regeneration are caused by the existence of long pores with irregular form of the channels. This conclusion points to the fact that the development of TEUF on the base of traditional technology of production of track-etched filters (44) is quite unpromising.

As follows from this figure, in contrast to TEUF of first type with practically constant selective layer thickness coinciding with the thickness of membrane, the TEUF of the second series (zone II) show a great variety of l_S values. Thus, along with TEUF with homogeneous structure [$l_S \sim 10\,\mu m$) we see UF membranes of intermediate type [$l_S \div (10-0.6)\,\mu m$] and also the highly asymmetric membranes ($l_S \sim 0.6-0.04\,\mu m$) coinciding by selective and permeable characteristics with membranes of Diaflo PM and Gelman Omega series.

Therefore one can see that the method (45) of obtaining membranes of the second type permits to produce TEUF of arbitrary structure which allows manufacturing membranes with optimal pore structure at the level of the best serial UF membranes.

Beside these examples, the rapid membrane structure analysis was successfully applied to the study of metal/ceramic membranes (47) and for the investigation of UF membrane modification (48).

CONCLUSION

As stated previously, the application of rapid analysis of membrane structure illustrates, as it seems to us, the indispensability of this method usage in the course of membrane development and manufacturing.

Really, as we saw, the revealment of the causes of defect emergence in composite polysulfonamide membranes required the analysis of approximately 30 membrane samples. If carried out by traditional methods of structure investigation this analysis would need the use of complex porometric and microscopic equipment with long and complicated procedure of data processing and rationalization. At the same time the use of rapid structure analysis allows a middle classification researcher to perform this work with the use of the simplest ultrafiltration and gel chromatographic equipment in 2 weeks.

The analysis of track-etched ultrafilters appeared to be more complicated either because of a large number (an order of a hundred) of these membranes or because of the prior unknown structure of membranes investigated. (Note: about 40% of membrane samples have been excluded from consideration as defective before the structure analysis.)

At the same time the use of rapid structure analysis made it possible for the group of three researchers to analyze on-line the structure of pilot membrane samples in the process of TEUF development.

List of Symbols

b	constant in eq. (3) (−)
C_b	bulk concentration (kg/m^3)
C_p	permeate concentration (kg/m^3)
D_2	parameter determining membrane defectness (−)
FRR	flux recovery ratio (−)
f_0	effective porosity (−)
f_{0i}	effective porosity of membrane layer with the thickness l_{Si} (−)
f(M)	differential numerical molecular weight distribution function (−)
f(R)	differential numerical pore size distribution (PSD) function (−)
$f_1(R)$	PSD function of membrane selective pores (−)
$f_2(R)$	PSD function of membrane defects (−)
J_1 and J_2	volume fluxes through selective and defective pores, respectively (m/s)
K	concentration rate (−)
K_1	constant in eq. (3) $(g/mol)^{-b}$
K_2	constant in eq. (12) $(g/mol)^{-0.76} m^2/s$
L	total membrane thickness (m)

l_S	selective layer thickness (m)
l_{Si}	thickness of membrane layer with effective porosity f_{0i} (m)
l_S^*	thickness of selective layer calculated with the arbitrary assumption that membrane effective porosity is 10%. (m)
M	molecular mass (weight) (kg/mol)
M_L	MWCO–molecular weight cut-off (kg/mol)
M_{01}	molecular weight corresponding to 10% retention (kg/mol)
R	pore radius (m)
R_h	mean hydrodynamic pore radius (m)
R_{hi}	mean hydrodynamic pore radius in membrane layer with thickness l_{Si} (m)
R_P	pore radius determined by Hagen–Poiseuille equation (m)
R_0	pore radius corresponding to the maximum of PSD function (m)
r_L	minimal Stokes' radius of protein molecule effectively retained by membrane (m)
r_S	Stokes' radius of protein molecule (m)
Δ	dispersion coefficient of retention curve (–)
Δp	trans-membrane pressure (Pa)
ΔR	value of pore radius decrease by gel layer (m)
λ_{cr}	"critical ratio" of minimal radius of protein molecule effectively retained by membrane to mean hydrodynamic pore radius (–)
Π_2	parameter determining membrane defectness in liquid displacement method (–)
σ	retention curve dispersion (–)
σ_0	dispersion of the pore size distribution function (–)
φ	observed retention coefficient (–)
$\varphi(M)$	membrane retention curve (–)
$\varphi[r(M)/(R -$	$\Delta R)] \equiv \varphi(\lambda)$ sieving function (–)
$\varphi^*(M)$	retention curve of defective membrane (–)

REFERENCES

1. Nakao, S. (1994) Determination of pore size and pore size distribution 3. Filtration membranes. *J. Memb. Sci.*, 96 (1–2): 131–165.
2. Baltus, R.E. (1997) Characterization of the pore area distribution in porous membranes using transport measurements. *J. Membr. Sci.*, 123 (2): 165–184.
3. Cherkasov, A.N. (1990) Selective ultrafiltration. *J. Membr. Sci.*, 50 (2): 109–130.
4. Cherkasov, A. and Chechina, V (2000) The use of calibration data for analysis of ultrafiltration membranes structure, 14 International Chemical and Process

Engineering CHISA-2000, Prague, Czech Republic, August 27–31, Summaries 2, 127.; CD-ROM of full texts, D 5.5, Prague, Czech Republic, August 27–31.
5. Blatt, W.F., Dravid, A., Michaels, A.S., and Nelsen, L.M. (1970) Solute polarization and cake formation in membrane ultrafiltration, causes, consequences, and control techniques. In *Membrane Science and Technology*; Flinn, J.E., ed.; Plenum Press: New York, 47–97.
6. Nakao, S., Wijmans, J.G., and Smolders, C.A. (1986) Resistance to the permeate flux in unstirred ultrafiltration of dissolved macromolecular solutions. *J. Membr. Sci.*, 26 (2): 165–178.
7. Van den Berg, G.B. and Smolders, C.A. (1989) The boundary layer resistance model for unstirred ultrafiltration. A new approach. *J. Membr. Sci.*, 40 (2): 149–172.
8. Vilker, V.L., Colton, C.K., and Smith, K.A. (1981) Concentration polarization in protein ultrafiltration. *AIChE J.*, 27: 632–645.
9. Cherkasov, A.N. (1985) Mechanism of selective separation of solutions in the process of ultrafiltration. *Kollodn. Zhurnal* (in Russian), 47 (2): 363–368.
10. Polotsky, A.E. and Cherkasov, A.N (2001) Mechanism of selective transport through ultrafiltration membranes from the standpoint of generalized sieving model, 41th Micro symposium on Polymer Membranes, Prague, Czech Republic, July 15 Summaries, 2, 41.
11. Cuperus, F.P., Bargeman, D., and Smolders, C.A. (1991) Characterization of anisotropic UF-membranes: top layer thickness and pore structure. *J. Membr. Sci.*, 61 (1): 73–83.
12. Kim, K.J., Fane, A.G., Fell, C.J.D., Suzuki, T., and Dickson, M.R. (1992) Quantative microscopic study of surface characteristics of ultrafiltration membranes. *J. Membr. Sci.*, 68 (1–2): 79–91.
13. Cherkasov, A.N., Tsareva, S.V., and Polotsky, A.E. (1995) Selective properties of ultrafiltration membranes from the standpoint of concentration polarization and adsorption phenomena. *J. Membr. Sci.*, 104 (1–2): 157–164.
14. Cherkasov, A.N., Polotsky, A.E., Gorelova, L.U., Zhemkov, V.P., and Belenky, B.G. (1981) The use of gel chromatography for ultrafiltration membranes characterization. *Kollodn. Zhurnal* (in Russian), 43 (4): 804–807.
15. Elford, W.J. (1937) Principles governing the preparation of membranes having graded porosities. The properties of "Gradicol" membranes as ultrafilters. *Trans. Faraday Soc.*, 33 (8): 1094–1106.
16. Cherkasov, A.N., Zhemkov, V.P., Mchedlishvili, B.V., Samohina, G.D., Buligin, A.N., Tretiakova, S.P., Kozlova, T.I., and Potokin, I.L. (1978) About the influence of particle-to-pore size ratio on membrane selectivity. *Kollodn. Zhurnal* (in Russian), 40 (6): 1155–1160.
17. Cherkasov, A.N., Petrova, V.N., and Polotsky, A.E. et al. (2000) The analysis of adsorption, selective, and permeable characteristics of track-etched ultrafilters of new type. 14 International Chemical and Process Engineering CHISA-2000, Prague, Czech Republic, August 27–31 Summaries, 2, 111., CD-ROM of full texts, D 3.4, Prague, Czech Republic, August 27–31.
18. Cherkasov, A.N. (1986) Dissertation for the degree of Doctor of Science. Technical-Scientific Association of USSR Academy of Science: Leningrad, USSR, 486.
19. Cherkasov, A.N. and Polotsky, A.E. (1995) Critical particle-to-pore size ratio in ultrafiltration. *J. Membr. Sci.*, 106 (1–2): 161–166.
20. Preusser, H.J. (1972) Die Ultrastruktur eingigerfeinporiger Membranfiltertypen. *Koll. Z. Z. Polym.*, 270 (1): 133–141.

21. Merin, U. and Cheryan, M. (1980) The structure of polysulfone ultrafiltration membranes. *J. Appl. Membr. Sci.*, 25 (9): 2139–2142.
22. Sarbolouki, M.N. (1984) Properties of asymmetric polyamide ultrafiltration membranes. 1. Pore size and morphology characterization. *J. Appl. Polym. Sci.*, 29 (3): 743–753.
23. Ferry, J.D. (1936) Statistical evaluation of sieve constants in ultrafiltration. *J. Gen. Physiol. J.D.*, 20: 95–104.
24. Cherkasov, A.N. and Polotsky, A.E. (1996) Resolving power of ultrafiltration. *J. Membr. Sci.*, 110 (1): 79–82.
25. Sleytr, U.B. and Sara, M. (1986) Ultrafiltration membranes with uniform pores from crystalline bacterial cell envelope layers (Mini-review). *Appl. Microbiol. Biotechnol.*, 25 (1): 83–90.
26. Weigert, S. and Sara, S. (1995) Surface modification of an ultrafiltration membrane with crystalline structure and studies of interaction with selected protein molecules. *J. Membr. Sci.*, 106 (1–2): 147–159.
27. Banks, W. and Sharples, A. (1966) Studies of desalination by reverse osmosis. III: Mechanism of solute rejection. *J. Appl. Chem.*, 16 (1): 28–32.
28. Sitharamaayya, S. and Mishura, P. (1988) The mechanism of ultrafiltration through cellulose acetate membranes. *Indian Chemical Engineering*, 30 (1): 72.
29. Ochoa, N.A., Prandanos, G., Palacio, L., Pagliero, C., Marchese, J., and Hernandez, A. (2001) Pore size distribution based on AFM imaging and retention of multidisperse polymer solutions. Characterization of polyrthersulfone UF membranes with dopes containing different PVP. *J. Membr. Sci.*, 187 (2): 227–237.
30. Lee, S., Park, G., Amy, G., Hong, S-K., Moon, S-H., Lee, D-H., and Cho, J. (2002) Determination of membrane pore size distribution using the fractional rejection of nonionic and charged macromolecules. *J. Membr. Sci.*, 201 (1–2): 191–201.
31. Michaels, A.S. (1980) Analysis and prediction of sieving curves for ultrafiltration membranes: A universal correlation? *Sep. Sci. Technol.*, 15 (6): 1305–1322.
32. Zydney, A.L., Aimar, P., Meirles, M., Pimbley, J.M., and Belford, G. (1994) Use of log-normal probability function to analyze membrane pore size distribution: functional form and discrepancies. *J. Membr. Sci.*, 91 (3): 293–298.
33. Ultrafiltrations–membrane ohne Fehlstellen. *Labor Praxis*, 2000, 24 (1): 62–64.
34. Niwa, M., Kawakami, H., Nagaoka, S., Kanamori, T., and Shinbo, T. (2000) Fabrication of an asymmetric polyimide hollow fibers with a defect-free surface skin layer. *J. Membr. Sci.*, 171 (2): 253–261.
35. Causserand, C., Aimar, P., Vilani, C., and Zamelli, T. (2002) Study of the effects of defects in ultrafiltration membranes on the water flux and the molecular weight cut-off. *Desalination*, 149 (2): 485–491.
36. Cherkasov, A.N. and Petrova, V.N., Ivanov, N.B. et al. (1991) Application of calibration method to determining the defects of ultrafiltration membranes. *Kollodn. Zhurnal* (in Russian), 53 (6): 1119–1126.
37. Cherkasov, A., Petrova, V., and Polotsky, A. (1999) The use of calibration method for investigation of defective ultrafiltration membranes. Book of Abstracts, Part 2, Euvromembrane, Leuven, September, 20–23, 481.
38. Ivanov, N.B., Zhemkov, V.P., Gromov, V.I., Cherkasov, A.N., Shshkov, L.A., and Mirni, V.P. (1986) The use of microfiltration method in the process of inactivated anti-influenza vaccine production. *Voprosi Virusologii* (in Russian), 4: 404–409.
39. Cherkasov, A.N., Zhemkov, V.P., Polotsky, A.E., Ivanov, N.B., and Potokin, I.L. (1984) Classification of ultrafiltration membranes on selective layer thickness. *Kollodn. Zhurnal* (in Russian), 46 (5): 980–985.

40. Nilson, J.L. (1990) Protein fouling of UF membranes: causes and consequences. *J. Membr. Sci.*, 52 (2): 121–142.
41. Cherkasov, A.N., Bon, A.I., Petrova, V.N., Tsareva, S.V., Andrianova, V.A., and Potokin, I.L. (1992) Usage of selective characteristics for analysis of the structure of ultrafiltration membranes. *Kollodn. Zhurnal* (in Russian), 54 (3): 157–162.
42. Cherkasov, A.N., Petrova, V.N., and Polotsky, A.E. et al. (2000) Selective and permeable characteristics of track etched ultrafilters. Book of Abstracts, Euvromembrane 2000, Jerusalem, Sept. 24–27. Tel Aviv: Target Tours, 2000, 215.
43. Cherkasov, A.N., Vlasova, O.L., Tsareva, S.V., Kolikov, V.M., and Mchedlishvili, B.V. (1990) Ultrafiltration on nuclear filters. *Kollodn. Zhurnal* (in Russian), 52 (3): 323–328.
44. Flerov, G.N. and Barashenkov, V.S. (1974) The practical usage of heavy ion beams. *Uspehi Fisicheskih Nayk* (In Russian), 114 (1): 351–373.
45. Zhdanov, D.S., Fursov, B.I., Krasavina, T.A., Tumanov, A.A., Mchedlishvili, B.V. and Nechaev, A.N. (2002) Method of asymmetric track-etched membranes production. Patent of Russia, 2179063, B01, D67/00, 69/00, April 23.
46. Tager, A.A. (1968) *Physics Chemistry of Polymers*; Himia: Moscow, Russia, 125–152.
47. Hataibe, E.V., Nechaev, A.N., Trusov, L.I., Svitsov, A.A., Pensin, R.A., Cherkasov, A.N., and Polotsky, A.E. (2002) Metalceramic membranes: structure and properties. 1. Structural, selective, and surface properties of ultrafiltration membranes. *Membrani* (in Russian), 16 (4): 10–14.
48. Sergeev, A.V., Nechaev, A.N., Petrov, N.V., Vlasov, S.V., and Mchedlishvili, B.V. (2004) The track membranes as the element of naostructures template synthesis. 1. The modified track membranes. *Membrani* (in Russian), 21 (1): 19–24.